

Energy gap of the high- T_c superconductor $\text{HgBa}_2\text{Ca}_2\text{Cu}_3\text{O}_{8+\delta}$ determined by point-contact spectroscopy

G. T. Jeong, J. I. Kye, and S. H. Chun

Department of Physics, Seoul National University, Seoul 151-742, Korea

Sergey Lee and S. I. Lee

Department of Physics, Pohang Institute of Science and Technology, Pohang, P. O. Box 135, Kyungbuk 790-600, Korea

Z. G. Khim

Department of Physics, Seoul National University, Seoul 151-742, Korea

(Received 6 January 1994)

Tunneling spectra of a polycrystalline bulk $\text{HgBa}_2\text{Ca}_2\text{Cu}_3\text{O}_{8+\delta}$ with $T_c = 132$ K have been measured by point-contact spectroscopy using a low-temperature scanning tunneling microscope. Unlike other high- T_c superconductors the conductance of this material shows a BCS-like gap structure with a relatively small smearing parameter Γ . Conductances with a linear density of states for $|eV| < \Delta$ and a small cusp at the gap are also observed. From a simple calculation based on the assumption that the surface is covered with a normal layer, we explained the linear dI/dV for $|eV| < \Delta$ and obtained two distinctively different energy gaps $\Delta = 48$ meV and 22 meV with the resultant $2\Delta/k_B T_c = 8.5$ and 3.9, respectively.

Recent discovery^{1,2} of Hg-Ba-Ca-Cu-O with its superconductive critical temperature increasing up to 165 K subjected to a high pressure³ has renewed the hope for the realization of superconductors with even higher critical temperature.

However, the basic underlying mechanism for the high- T_c superconductor still remains unclear and is the subject of intensive study both experimentally and theoretically. Electron tunneling measurements proved to be a very powerful method to investigate the superconducting properties due to its ability to probe the local density of states (DOS) from which one can determine the energy gap as well as the underlying interaction through, for example, the Eliashberg equation.⁴ Furthermore due to its directional probing nature, electron tunneling spectroscopy is frequently employed for the study of the symmetry in the energy gap by performing a directional tunneling on a single-crystal superconductor.⁵ However, tunneling data⁶ on high- T_c superconductors so far are rather scattered due to the lack of control of tunneling barrier. Poor quality of natural oxide and short coherence length in high- T_c oxide superconductors make the approach of using the planar-type tunnel junction almost impossible frequently producing complicated and reduced energy gap structures. Recently Chen *et al.*⁷ reported $\Delta = 15$ meV and $2\Delta/k_B T_c = 3.6$ for $\text{HgBa}_2\text{CuO}_{4+\delta}$ with $T_c = 92$ K.

In this work, we performed an electron tunneling measurement for a bulk $\text{HgBa}_2\text{Ca}_2\text{Cu}_3\text{O}_{8+\delta}$ by a point-contact spectroscopy using a low-temperature scanning tunneling microscope (LTSTM). Like many other high- T_c oxide superconductors, $\text{HgBa}_2\text{Ca}_2\text{Cu}_3\text{O}_{8+\delta}$ shows a large energy gap with the resulting energy gap to critical temperature ratio $2\Delta/k_B T_c = 8.5$. In addition, we also observed an evidence of another smaller energy gap $\Delta = 22$ meV in the tunneling conductance.

Tunneling measurement for a polycrystalline bulk $\text{HgBa}_2\text{Ca}_2\text{Cu}_3\text{O}_{8+\delta}$ with the critical temperature 132 K was made by a point-contact spectroscopy. Samples were synthesized in two steps, that is production of precursor pellet and formation of the superconducting samples inside the quartz tubes. The precursor pellets of Ba-Ca-Cu-O were prepared by mixing the appropriate amount of nitrates: $\text{Ba}(\text{NO}_3)_2$, $\text{Ca}(\text{NO}_3)_2 \cdot 4\text{H}_2\text{O}$, and $\text{Cu}(\text{NO}_3)_2 \cdot 2.5\text{H}_2\text{O}$. After the heat treatment of this reagents, a stoichiometric amount of HgO was added to the precursor and mixed in a glove box in nitrogen atmosphere. Then the sample was heated with a high Hg vapor pressure of about 200 atm. The oxygenation of samples was carried out in flowing oxygen at 300°C for 20 h. X-ray-diffraction measurement shows a well-defined diffraction pattern with a minor BaCuO_2 impurity phase. The zero-resistance temperature of the sample was 132 K obtained from the four-probe resistance measurement.

The mechanical part of the low-temperature STM system was mounted in a long cylindrical stainless tube filled with He gas to reduce the thermal drift effect. Helium exchange gas pressure was kept at about 1 mTorr, high enough to maintain a thermal equilibrium during the tunneling experiment and also low enough to prevent an electric discharging effect. A differential lever screw was employed for the coarse approach of the tip to the sample. The mechanical part in the cylindrical tube was then immersed in liquid helium cryostat. The maximum scan length of the constructed LTSTM along lateral and vertical directions 4.2 K was about 0.8 μm and 0.2 μm , respectively. A mechanically wire drawn Pt-Rh tip turned out to be more stable than the electrochemically polished W tip. The typical radius of the Pt-Rh tip used in this experiment is estimated to be about 0.2 μm from the scanning electron microscopy image. Successful imaging of highly oriented pyrolytic graphite at 4.2 K

with the Pt-Rh tip also indicates that the actual tunneling takes place at a local point on the tip.

To overcome the possible degradation of the sample surface, the $\text{HgBa}_2\text{Ca}_2\text{Cu}_3\text{O}_{8+\delta}$ sample surface was scraped with a file just before mounting on the sample stage of LTSTM. Immediately after mounting the sample, the cylinder was filled with helium exchange gas. The air exposure time of the scratched surface was less than 20 min.

The rough surface of the scraped sample prevented any continuous scanning for the surface image. Therefore the actual tunneling measurement was done in a point-contact tunneling style. A stable tunneling current was obtained for the tunneling resistance of the order of 1 G Ω at 4.2 K. To examine the conductance of a nearby spot, we retracted and moved the tip to the new spot. Tunneling spectroscopy was performed using the usual lock-in technique. The magnitude of the modulation voltage was 1.65 mV with the sweep rate of about 10 s. Even with the feedback signal turned off during the tunneling measurement, the tunnel junction remained stable for at least several minutes at 4.2 K.

Figure 1 shows four representative tunneling conductance dI/dV vs V curves obtained from four different spots in the $\text{HgBa}_2\text{Ca}_2\text{Cu}_3\text{O}_{8+\delta}$ bulk sample at 4.2 K. For clarity, zeros of conductance of Figs. 1(b), 1(c), and 1(d) are shifted by 1 successively.

Common features in the conductance of high- T_c super-

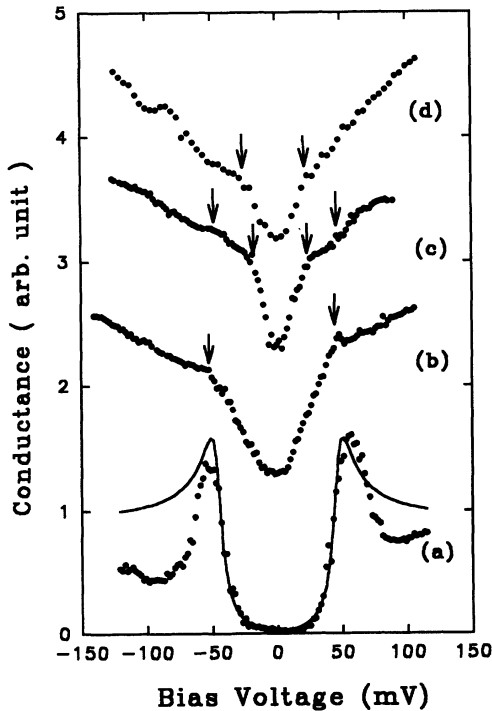


FIG. 1. Experimental conductances (dot) obtained from four different locations at 4.2 K. Curve (a) shows a good agreement with the calculated conductance (solid line) using a smeared BCS density of states ($\Delta_0 = 48$ meV and $\Gamma = 5$ meV). Curves (b), (c), and (d) obtained from different spots show a small cusp at the gap edge (indicated by arrows) and linear dI/dV for $|eV| < \Delta$. For clarity, zeros of conductance of (b), (c), and (d) are shifted by 1 successively.

conductors are that (i) there appears a pronounced asymmetry depending on the polarity,^{8,9} (ii) dI/dV peaks show a significant broadening,¹⁰ and (iii) the background in dI/dV shows a linearly increasing^{11,12} and strongly temperature-dependent conductance background.¹³

Tunneling conductance of $\text{HgBa}_2\text{Ca}_2\text{Cu}_3\text{O}_{8+\delta}$, in general, also shows similar features mentioned above. The conductance curve of Fig. 1(a) is by far the most BCS-like dI/dV curve obtained from high- T_c superconductors so far except that there is a significant broadening of the peak (peak voltage 54 mV) near the gap region and a large dip just above the gap. Within 0.5 μm from this spot A, we obtained a similar and reproducible BCS-like conductance. Zero-bias conductance is less than 5% of the normal conductance. Near-zero conductance for $|eV| < \Delta$ virtually excludes the possibility of gap anisotropy being responsible for the broadening of the dI/dV peak at the gap edge. The calculated dI/dV curve [solid line in Fig. 1(a)] using a smeared density of states¹⁴

$$N_s(E) = \text{Re} \left\{ \frac{E}{\sqrt{E^2 - (\Delta + i\Gamma)^2}} \right\}, \quad (1)$$

with energy-gap parameter $\Delta = 48$ meV, pair breaking parameter $\Gamma = 5$ meV ($\Gamma \cong 0.1\Delta$), and also including the thermal smearing effect, shows good agreement with the experimental curve up to the gap region. The energy gap to T_c ratio $2\Delta/k_B T_c$ is 8.5, somewhat larger than the commonly accepted value of other high-temperature superconductors (HTSC's). The introduction of the pair breaking parameter Γ is rather arbitrary. However, if one interprets $\Gamma = \hbar/\tau$ as the result of the lifetime effect of the Cooper pair, τ is about $\sim 8 \times 10^{-13}$ s for the present sample. The dip structure just above the gap is a common feature of the HTSC and presumably it is associated to the intrinsic interaction of the HTSC. Quantitative analysis for the size of the dip structure requires the normalization of the conductance data. But as mentioned above, the normalization procedure was impossible due to the temperature dependence of the normal background.

Tunneling conductances of Figs. 1(b), 1(c), and 1(d) obtained at different spots (several μm away from spot A) show quite a different behavior compared to the conductance of Fig. 1(a). Aside from the strong asymmetry in dI/dV , noticeable differences are that these conductances show (i) a small cusp at the gap edge and more importantly (ii) almost a linear dI/dV for $|eV| < \Delta$. The asymmetry of dI/dV observed in this study is a common feature observed in high- T_c superconductors.

If we interpret the cusp of Fig. 1(b) as a result of the energy gap, the energy gap parameter inferred from a similar simulation as above with the smearing effect is ~ 40 meV, which is about 20% less than the value obtained from Fig. 1(a). Of course, the simulated dI/dV curve does not reproduce the linear density of states inside the energy gap. The conductance obtained at a spot C ($\sim 0.1 \mu\text{m}$ away from spot B) show noticeable changes of slope in dI/dV at bias 21 mV and 51 mV, which can be interpreted as an indication of double gaps as shown in Fig. 1(c). At a different spot D which is also in the

vicinity of spot *B*, we have observed a conductance with a smaller energy gap only as shown in Fig. 1(d). If one assumes that the slopes change in the dI/dV is due to the gap in this material, estimated sizes of the energy gap counting the smearing effect are $\Delta_1 = 19.7$ meV and $\Delta_2 = 46$ meV, the value which is very close to the one obtained from the BCS-like dI/dV curve. Thus it seems there are at least two energy gaps either due to gap anisotropy or due to existence of other impurity phases in this material. However, even with two gaps in this material, calculated conductances cannot mimic the experimentally observed linear conductance inside the gap region, shown in Figs. 1(b), 1(c), and 1(d). It is likely that these spots are covered with a normal material thus reducing the energy gap through the proximity effect as well as generating the asymmetry.

In order to explain the linear conductance observed inside the energy gap region, we assumed that part of the $\text{HgBa}_2\text{Ca}_2\text{Cu}_3\text{O}_{8+\delta}$ surface is covered with a normal layer with its thickness x following a Gaussian distribution $\propto \exp(-x^2/2\sigma^2)$. With the use of de Gennes boundary condition¹⁵ for the normal-metal-superconductor interface in the absence of an external field, we have taken the proximity-induced energy gap at the tunneling surface of the normal layer with thickness x as

$$\Delta(x) = \Delta_0 \exp(-x/\xi_N), \quad (2)$$

where Δ_0 and ξ_N are the energy gap at the *S*-layer surface and the coherence length of the *N* layer, respectively. The average tunneling density of states for a distributed *N*-layer thickness up to d in this model is then

$$N_N(E) = \frac{1}{d} \int_0^d dx \exp\left(\frac{-x^2}{2\sigma^2}\right) \times \text{Re} \left\{ \frac{E}{\sqrt{E^2 - [\Delta(x) + i\Gamma]^2}} \right\}. \quad (3)$$

The calculated conductance employing Eq. (3) with a reasonable choice of parameter values, maximum normal layer thickness $d = 200$ nm, thickness distribution parameter $\sigma = 70$ nm, and coherence length of normal layer $\xi_N = 100$ nm, together with the experimental conductance curve is shown in Fig. 2(a). Here the *S*-layer energy gap and pair breaking parameter values are chosen as $\Delta_0 = 48$ meV and $\Gamma = 0.1\Delta(x)$, the value obtained from the simulation of the BCS-like conductance of Fig. 1(a). Aside from the asymmetry and background above the gap edge, the agreement is very good inside the gap region. The slope of the conductance as well as the peak position of dI/dV matches very well with the experimental conductance curve. For the calculation of the double gap conductance curve of Fig. 1(c), we have used the tunneling density of states given by Eq. (3), portion (r) of which is from the normal layer backed by $\text{HgBa}_2\text{Ca}_2\text{Cu}_3\text{O}_{8+\delta}$ with a larger energy gap $\Delta_{01} = 48$ meV and the remaining portion $(1 - r)$ from the normal layer backed by $\text{HgBa}_2\text{Ca}_2\text{Cu}_3\text{O}_{8+\delta}$ with a smaller energy gap $\Delta_{02} = 22$ meV. The calculated conductance curve with this combined density of states with $r = 0.5$ also shows a good agreement with the experimental curve as shown in Fig. 2(b). The reasonably good agreement between experimental and calculated conductance again supports our assumption that there are two energy gaps in the $\text{HgBa}_2\text{Ca}_2\text{Cu}_3\text{O}_{8+\delta}$ material, $\Delta_1 = 48$ meV and $\Delta_2 = 22$ meV.

In order to see the possibility of another low- T_c phase being involved for the multiple gap, we measured the magnetic susceptibility of the sample with a Quantum Design SQUID magnetometer. As shown in Fig. 3, the critical temperature is 132 K and more importantly there is no detectable trace of any other phase in the susceptibility measurement. Although one still cannot rule out the possibility of other impurity phases being responsible for the smaller gap, the absence of any impurity phase in

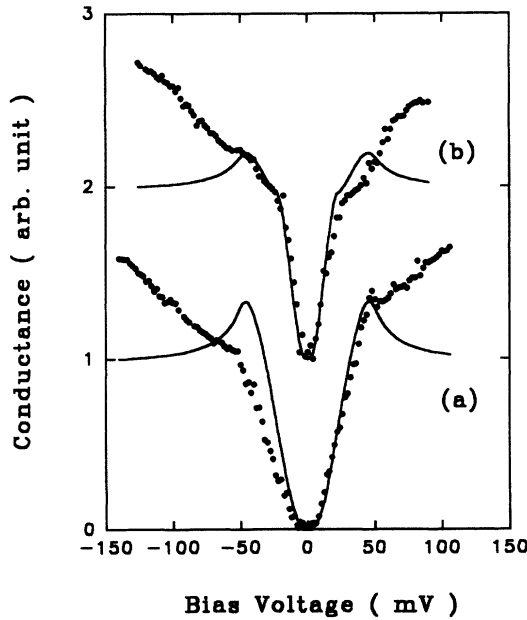


FIG. 2. Calculated conductance (solid line) based on the proximity-induced energy gap in a normal layer on the surface of the superconductor shows a good agreement with experimental conductances (dot), (a) normal layer backed by a superconductor with $\Delta_0 = 48$ meV, and (b) normal layer backed by superconductors with $\Delta_{01} = 48$ meV and $\Delta_{02} = 22$ meV.

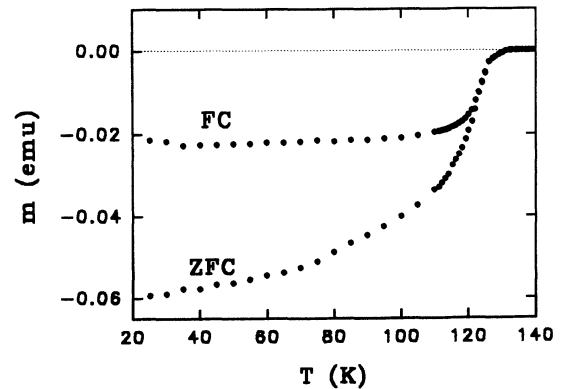


FIG. 3. Magnetic susceptibility vs T for $\text{HgBa}_2\text{Ca}_2\text{Cu}_3\text{O}_{8+\delta}$ samples shows $T_c = 132$ K. No other phase is detectable in the susceptibility measurement.

the magnetic-susceptibility measurement is interpreted as an indication that the observed two different gaps are due to the gap anisotropy in this material reflected in the normal layer through the proximity effect.

In summary, we have observed a BCS-like gap structure in the tunneling conductance of a bulk $\text{HgBa}_2\text{Ca}_2\text{Cu}_3\text{O}_{8+\delta}$ by a point-contact spectroscopy using a low-temperature STM technique. The fitted gap parameter and energy gap to critical temperature ratio obtained through a simulation with a smeared density of states are $\Delta_1 = 48$ meV and $2\Delta/k_B T_c = 8.5$, respectively. At other spots in the sample, we have also observed distinctively different tunneling conductances which can be characterized with small cusps at gap edges and a linearly increasing dI/dV for $|eV| < \Delta$. With the assumption that these spots are covered with a normal layer of a distributed thickness, we have explained the almost linearly increasing conductance for $|eV| < \Delta$, the

behavior which is commonly observed in other high- T_c superconductors as well, and obtained two energy gap parameters, $\Delta_1 = 48$ meV and $\Delta_2 = 22$ meV with the resultant $2\Delta/k_B T_c = 8.5$ and 3.9, respectively.

The nature of the normal layer on the $\text{HgBa}_2\text{Ca}_2\text{Cu}_3\text{O}_{8+\delta}$ surface assumed in the analysis of tunneling conductances in this work is not well known at present. It is also not clear whether the origin of the two gaps observed in this work is due to the gap anisotropy or due to the multiple phase of the sample. Nevertheless, the satisfactory agreement between experimental and calculated conductance curves indicates a strong possibility that $\text{HgBa}_2\text{Ca}_2\text{Cu}_3\text{O}_{8+\delta}$ has an s -wave-like energy gap with two distinctive gaps. Directional tunneling measurement on a single-crystal Hg-Ca-Ba-Cu-O is necessary for further understanding on the symmetry of the energy gap in this material.

¹ S. N. Putilin, E. V. Antipov, O. Chmaissem, and M. Marezio, *Nature* **362**, 226 (1993).

² A. Schilling, M. Cantoni, J. D. Guo, and H. R. Ott, *Nature* **363**, 56 (1993).

³ L. Gao, Y. Y. Xue, F. Chen, Q. Xiong, R. L. Meng, D. Ramirez, C. W. Chu, J. H. Eggert, and H. K. Mao (unpublished).

⁴ E. L. Wolf, *Principles of Electron Tunneling Spectroscopy* (Oxford University Press, New York, 1985).

⁵ J. Kane, Q. Chen, K.-W. Ng, and H.-J. Tao, *Phys. Rev. Lett.* **72**, 128 (1994).

⁶ See T. Hasegawa, H. Ikuta, and K. Kitazawa, in *Physical Properties of High Temperature Superconductors III*, edited by D. M. Ginsberg (World Scientific, Singapore, 1992).

⁷ J. Chen, J. F. Zasadzinsky, K. E. Gray, J. L. Wagner, and D. G. Hinks (unpublished).

⁸ J. M. Valles, Jr., R. C. Dynes, A. M. Cucolo, M. Gurvich, L. F. Schneemeyer, J. P. Garno, and J. V. Waszczak, *Phys. Rev. B* **44**, 11 986 (1991).

⁹ S. Martin, E. S. Hellman, A. Kussmaul, and E. H. Hartford,

Jr., *Phys. Rev. B* **47**, 14 510 (1993).

¹⁰ A. P. Fein, J. R. Kirtely, and M. W. Shafer, *Phys. Rev. B* **37**, 9738 (1988).

¹¹ M. Gurvitch, J. M. Valles, Jr., A. M. Cucolo, R. C. Dynes, J. P. Garno, L. F. Schneemeyer, and J. V. Waszczak, *Phys. Rev. Lett.* **63**, 1008 (1989).

¹² F. Sharifi, A. Pargellis, and R. C. Dynes, *Phys. Rev. Lett.* **67**, 509 (1991).

¹³ H. J. Tao, A. Chang, Farun Lu, and E. L. Wolf, *Phys. Rev. B* **45**, 10 622 (1992).

¹⁴ Although it is a common practice to attribute the broadening of conductance to the quasiparticle lifetime effect, it can also be attributed to the pair breaking effect as has been adopted in this work. Both approaches produce nearly identical results. R. C. Dynes, V. Narayanamurti, and J. P. Garno, *Phys. Rev. Lett.* **41**, 1509 (1978); Zhao Shifeng, Tao Hongjie, Chen Yinfei, Yan Yifen, and Yang Qiansheng, *Solid State Commun.* **67**, 1179 (1988).

¹⁵ P. G. de Gennes, *Superconductivity of Metals and Alloys* (Benjamin, New York, 1966).